The Structure of CrFeTi$_2$O$_7$

I. E. GREY AND W. G. MUMME

CSIRO Division of Mineral Chemistry, P.O. Box 124, Port Melbourne, Victoria 3207, Australia

The phase CrFeTi$_2$O$_7$ has been synthesized and is monoclinic, $P2_1/a$, $a = 7.032(3)$ Å, $b = 5.000(2)$ Å, $c = 14.425(6)$ Å, $\beta = 116.59(4)°$. It is isostructural with the compound Cr$_2$Ti$_2$O$_7$. The structure is based on distorted hexagonal close packing of oxygen atoms, with the metal atoms occupying particular octahedral interstices to give a complex arrangement of octahedra joined by the sharing of corners, edges and faces. For one of the metal atom sites in the structure there is a 15 % disorder for which possible origins are discussed. CrFeTi$_2$O$_7$ is a member of the homologous series of compounds A$_2$B$_{n-2}$O$_{2n-1}$ (A = Cr, Fe; B = Ti, Zr) whose structures are closely related to that of α-PbO$_2$, and may be considered to derive from it by the application of crystallographic shear.

Introduction

The Cr$_2$O$_3$–TiO$_2$ phase system has been extensively studied (*1–4*) and a number of discrete phases of general formula Cr$_2$Ti$_{n-2}$O$_{2n-1}$, $n = 3$, 4, 6–9 have been prepared. Phases corresponding to $n = 6$–9 have been characterized by X-ray diffraction techniques. These compounds are isomorphous with members of the homologous series Ti$_n$O$_{2n-1}$ (*5*) and V$_n$O$_{2n-1}$ (*6*). The structures of these compounds are closely related to that of rutile and may be derived from it by crystallographic shear (*7*).

For the case $n = 4$, Cr$_2$Ti$_2$O$_7$ was first identified by Hamelin (*1*) as a discrete compound, not part of the Andersson phase series (*2*). Mention has been made of the difficulty of growing single crystals suitable for X-ray work, for this highly refractory material (mp = 1980°C), and hitherto the structure of Cr$_2$Ti$_2$O$_7$ has remained unknown.

In a study of the Fe$_2$O$_3$–Cr$_2$O$_3$–TiO$_2$ system (*3*), Kwestroo and Roos reported that up to 66 mole % Cr may be replaced by Fe in Cr$_2$Ti$_2$O$_7$ without the structure undergoing any change. We have found that replacement of Cr by Fe lowers the melting point of the (Cr,Fe)$_2$Ti$_2$O$_7$ species. For the case of 50 mole % replacement of Cr by Fe we have obtained single crystals of CrFeTi$_2$O$_7$ by sintering the reaction mixture at 1500°C. In this paper the structure of this compound as determined by X-ray methods is described.

Experimental

The stoichiometric mixture Fe$_2$O$_3$:Cr$_2$O$_3$: 4TiO$_2$ was intimately mixed, pressed into a pellet and heated in air at 1500°C for 100 hr then quickly cooled to room temperature. Crystals suitable for X-ray analysis grew from the surface of the sinter in the form of black, shiny needles. The unit cell parameters listed in Table I resulted from a least-squares treatment of powder data obtained with a Philips powder diffractometer fitted with a graphite monochromator, using Cu$K\alpha$ radiation. Potassium chloride, $a = 6.2931$ Å, was used as an internal standard, and slow scan

TABLE I

CRYSTALLOGRAPHIC CONSTANTS FOR CrFeTi$_2$O$_7$

Symmetry	Monoclinic
Unit Cell	$a = 7.032$ ($\pm$ 0.003) Å
	$b = 5.000$ ($\pm$ 0.002) Å
	$c = 14.425$ ($\pm$ 0.006) Å
	$\beta = 116.59$ ($\pm$ 0.04)°
Systematic extinctions	$h0l, h \neq 2n$
	$0k0, k \neq 2n$
Space group	$P2_1/a$
D_x	4.62 g cm^{-3}
Z	4

rates (1/4°/min) were used to ensure high precision in the data.

For the structure determination, a crystal measuring $0.01 \times 0.01 \times 0.1$ mm was mounted along its needle axis (b), and intensity data hkl for the levels $k = 0$, 1, 2 and 3 were obtained by the integrated Weissenberg technique with the use of filtered copper radiation. Two data sets were collected, using different exposure times, to extend the range of measured intensities. The intensities were measured visually by two independent observers, then averaged. The reduction to structure amplitudes and all subsequent computing was made on an Elliott 803 computer, at the CSIRO Division of Mineral Chemistry, with the programming system devised by Daly, Stephens, and Wheatley (8) and kindly made available to the authors by Dr. P. J. Wheatley. Interlayer scaling for the four levels of data was adjusted after each least-squares refinement cycle. (The scaled observed data and structure amplitudes calculated from the final model are available.[1]) Scattering curves for metals, M, and oxygen, O^{2-}, were taken from International Tables for X-Ray Crystallography (1962, pp. 201 ff). It was assumed that iron, chromium and titanium randomly occupied the metal sites, and so $f(M) = 1/4(f\,Cr^{3+} + f\,Fe^{3+} + 2f\,Ti^{4+})$.

Determination of the Structure

The powder diffractogram for $CrFeTi_2O_7$ bore a close resemblance to that for V_3O_5 (6). The unit cells for the two compounds have monoclinic symmetry with a common unique 5 Å axis, b. This suggested a similar distribution of metal atoms in layers at $y \simeq 1/4$ and 3/4. On this basis the sharpened three-dimensional Patterson map was solved for the positions of four independent metal atoms in general positions. The four metal atoms were used to phase reflections and generate a three-dimensional Fourier synthesis from which approximate positions for the seven oxygen atoms were obtained. The positions of the atoms were initially refined by difference Fourier syntheses to an agreement factor, $R = 14\%$. From this point refinement was carried out by a number of least-squares cycles, varying coordinates and isotropic temperature factors. After several cycles R reached a steady state value of 10.8%. A three-dimensional Fourier map was generated from which it was observed that the peak height corresponding to one of the metals, M_1, was approxi-

[1] Lodged with NAPS.

TABLE II

VARIATION OF R FACTOR WITH DISORDER OF METAL, M_1

Percentage disorder of M_l	R
0	10.8
10	9.1
15	8.8
20	9.1
30	10.9

mately 80% of the peak heights for the other three metal atoms. In addition, the Fourier indicated a residual peak, M_3, for which the peak height was 20% of the average height of the three metal atom peaks. Calculation of bond distances and angles between M_3 and its oxygen neighbours showed that the site was octahedrally coordinated, with bond lengths similar to those obtained for the other metal atoms. Thus it provides a possible alternative to M_1 for metal atom occupation. Refinement to a steady state R value was therefore carried out for a number of different values for the occupancy of these sites. The results shown in Table II indicate approximately 15% disorder of metal atoms from site M_1 to site M_3. The final value for R for all observed reflections, and allowing 15% occupation of site M_3, was 8.8%. In view of this disorder in the structure, it was not possible to determine whether different metal atom types were ordered. Random occupancy of the independent metal atom sites by iron, chromium and titanium was therefore assumed.

Description of Structure

The following section relates to a description of the ideal structure of $CrFeTi_2O_7$ and ignores the disorder in the structure which will be discussed in a later section. A ball and spoke representation of the structure as viewed down [010] is shown in Fig. 1. The oxygen atoms form a distorted hexagonal close packed lattice with the metal atoms occupying certain octahedral interstices to give a complex arrangement of octahedra mutually joined by sharing corners, edges and faces. The octahedra associated with metal atoms M_1 and M_2 (see Table III) form binuclear units by sharing a common face. The
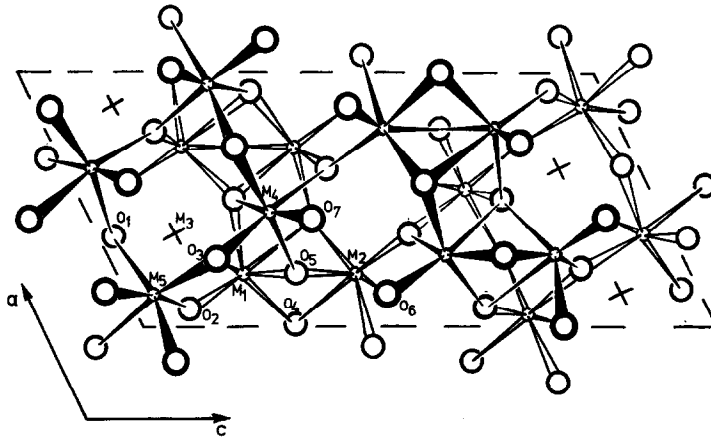
FIG. 1. Ball and spoke representation of the structure of $CrFeTi_2O_7$, viewed down b. Oxygen bonds to metal atoms at $y \simeq 3/4$ are represented by solid tapers; those to metal atoms at $y \simeq 1/4$ are shown by open tapers. Disordered metal atom sites M_3 are denoted by crosses.

face-shared pairs link into infinite stepped chains along [100] by edge sharing. The chains further link into sheets parallel to (001) by edge sharing with a third type of octahedron, containing M_4. Pairs of such sheets, related by a centre of symmetry, share corners to build up slabs of V_3O_5-type structure (9), parallel to (001). These V_3O_5 type slabs connect via corner sharing with sheets of α-PbO_2 structural type (10) containing metals M_5 to complete the structure. In Fig. 2 is shown an idealized representation of the structure as viewed down [010]. The structures for V_3O_5 and α-PbO_2 (high pressure form of TiO_2 (11)) are also shown in the same projection. $CrFeTi_2O_7$ is effectively a 1:1 intergrowth of

$CrFeTiO_5$, of V_3O_5 structure type, and TiO_2 of α-PbO_2 structure type. Interatomic distances associated with all the metal atoms are given in Table IV. Individual M–O bond lengths vary between 1.82 and 2.12 Å for M_2, M_4 and M_5 while the disordered sites M_1 and M_3 have somewhat more distorted octahedra; M–O

TABLE III

FRACTIONAL ATOMIC COORDINATES AND THERMAL PARAMETERS
(e.s.d. in brackets)

Atom	x	y	z	$B(\text{Å}^2)$
M_1	0.2138(12)	0.249(4)	0.2190(6)	1.1(1)
M_2	0.2114(13)	0.263(4)	0.4137(6)	2.1(1)
M_3	0.3741(83)	0.284(20)	0.1359(38)	1.5(11)
M_4	0.4532(14)	0.733(4)	0.3183(6)	1.2(1)
M_5	0.1289(12)	0.739(4)	0.0460(6)	1.8(1)
O_1	0.3610(58)	0.576(11)	0.0244(27)	2.6(8)
O_2	0.0687(47)	0.434(9)	0.0960(22)	1.1(6)
O_3	0.2730(56)	0.907(8)	0.1849(28)	1.3(6)
O_4	0.0586(60)	0.110(9)	0.2652(28)	2.7(8)
O_5	0.2112(66)	0.553(8)	0.3118(30)	1.6(6)
O_6	0.1265(62)	0.895(10)	0.4547(28)	2.7(8)
O_7	0.4295(50)	0.081(8)	0.3862(22)	1.0(6)
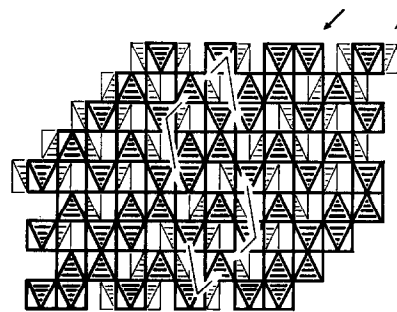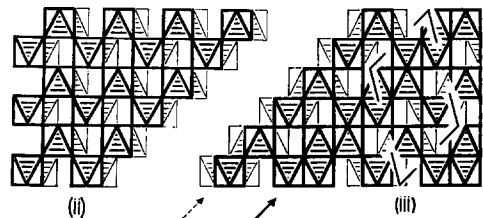
FIG. 2. Idealized view of structures according to the representation developed by Andersson and Galy (17). (i) ideal structure of $CrFeTi_2O_7$, viewed down b; arrows indicate direction of shear; (ii) α-PbO_2 structure viewed down c; (iii) V_3O_5 structure viewed down b.

TABLE IV

INTERATOMIC DISTANCES (Å)
(e.s.d. in brackets)

Metal–Oxygen					Metal–Metal
M_1 octahedron	M_2 octahedron	M_3 octahedron	M_4 octahedron	M_5 octahedron	
M_1-O_2 1.85(4)	M_2-O_4 2.12(4)	M_3-O_1 2.14(9)	M_4-O_3 1.97(4)	M_5-O_1 1.99(5)	M_1-M_2 (face) 2.82(2)
$-O_3$ 1.88(4)	$-O_5$ 2.06(4)	$-O_1'$ 2.39(9)	$-O_4$ 1.98(4)	$-O_1'$ 1.97(5)	$-M_2$ (edge) 3.37(2)
$-O_4'$ 1.98(4)	$-O_6$ 2.10(4)	$-O_2$ 2.09(8)	$-O_5$ 1.89(4)	$-O_1''$ 1.98(5)	
$-O_5$ 2.03(4)	$-O_6'$ 1.84(4)	$-O_2'$ 2.02(8)	$-O_5'$ 2.14(4)	$-O_2$ 1.82(4)	M_4-M_1 (edge) 3.06(2) 2.93(2)
$-O_7$ 2.36(4)	$-O_7$ 2.00(4)	$-O_3$ 2.24(9)	$-O_6$ 1.90(5)	$-O_2'$ 2.08(4)	$-M_2$ (edge) 3.02(2) 3.05(2)
	$-O_7'$ 1.97(4)	$-O_4$ 1.75(9)	$-O_7$ 2.04(4)	$-O_3$ 1.98(4)	
O_2-O_3 3.00(5)					M_5-M_5 (edge) 2.94(2) 3.11(2)
O_2-O_4 3.12(6)	O_4-O_5 2.56(6)	O_1-O_1' 2.86(6)	O_3-O_4 3.00(6)	O_1-O_1'' 2.48(6)	
$-O_4'$ 2.95(6)	$-O_6$ 2.70(6)	$-O_2$ 2.77(6)	$-O_5$ 2.72(6)	$-O_2$ 2.80(6)	M_3-M_5 (face) 2.63(7)
$-O_5$ 2.87(6)	$-O_7$ 2.56(6)	$-O_2'$ 2.89(6)	$-O_5'$ 2.80(6)	$-O_2'$ 2.69(6)	$-M_5$ (edge) 3.17(7)
O_3-O_4 2.80(6)	$-O_7'$ 2.70(6)	$-O_4$ 3.29(6)	$-O_7$ 2.75(5)	$-O_3$ 2.78(6)	
$-O_4'$ 2.85(6)	O_5-O_6' 3.14(6)	$O_1'-O_2$ 2.69(6)	O_4-O_5 2.58(6)	$O_1'-O_1'$ 2.86(6)	
$-O_7$ 2.74(5)	$-O_7$ 2.72(6)	$-O_2'$ 3.12(6)	$-O_5'$ 3.07(6)	$-O_2$ 2.77(6)	
O_4-O_5 2.56(6)	$-O_7'$ 2.76(6)	$-O_3$ 2.86(6)	$-O_6$ 2.70(6)	$-O_2'$ 2.73(6)	
$-O_7$ 2.70(6)	O_6-O_6' 2.99(6)	O_2-O_3 3.00(5)	O_5-O_6 2.73(6)	$-O_3$ 3.12(6)	
$O_4'-O_5$ 2.58(6)	$-O_7$ 2.92(6)	$-O_4$ 2.95(6)	$-O_7$ 3.00(6)	$O_1''-O_2'$ 2.89(6)	
$-O_7$ 2.56(6)	$-O_7'$ 2.87(6)	$O_2'-O_3$ 3.00(5)	$O_5'-O_6$ 2.93(6)	$-O_3$ 2.86(6)	
O_5-O_7 2.76(6)	$O_6'-O_7$ 2.93(6)	$-O_4$ 3.12(6)	$-O_7$ 2.73(6)	O_2-O_2 2.58(5)	
	$-O_7'$ 2.95(6)	O_3-O_4 2.85(6)	O_6-O_7 2.70(6)	$-O_3$ 2.77(5)	

distances vary between 1.85 and 2.36 Å for M_1 and between 1.75 and 2.39 Å for M_3. In Table V the averaged M–O bond lengths for metals M_1, M_2, M_4 and M_5 are compared with the involvement of their M–O bonds in corner, edge and face

sharing. Also listed in Table V is the averaged coordination number for the six oxygens associated with each metal, the effective oxygen ionic radii, calculated using the data of Shannon and Prewitt (12), and the resulting effective metal

TABLE V

Metal	Bridging involved			Averaged M–O distance	Averaged Oxygen coord.	Effective oxygen ionic radius	Effective metal ionic radius
	Corner	Edge	Face				
M_1	$2 \times M_1$ $2 \times M_5$	M_2 $2 \times M_4$	M_2	2.01	3.67	1.373	0.64
M_2	$3 \times M_2$ $2 \times M_4$	M_1 $2 \times M_4$	M_1	2.01	3.67	1.373	0.64
M_4	$2 \times M_1$ $3 \times M_2$ $2 \times M_4$ M_5	$2 \times M_1$ $2 \times M_2$		1.99	3.67	1.373	0.62
M_5	$3 \times M_1$ M_4 $4 \times M_5$	$2 \times M_5$		1.97	3.00	1.36	0.61

ionic radii. The metal ionic radii, which should be constant if Cr, Fe and Ti are randomized, are shorter by approximately 0.03 Å for metal atoms M_4 and M_5 as compared with metal atoms M_1 and M_2. This may be indicative of the presence of the Ti^{4+}, $r = 0.615$ Å, in sites M_4 and M_5 and the preference of Cr^{3+} and Fe^{3+}, $r_{av} = 0.64$ Å, for the face-shared octahedral sites M_1 and M_2, which are similar to those in the corundum structures (13, 14).

The face-sharing sites M_1 and M_2 exhibit a net repulsion of metal atoms across the shared face with $M_1–M_2 = 2.82$ Å as compared with 2.3 Å for ideal hexagonal close packing of the oxygen layers. The value is actually intermediate between 2.65 Å as found in Cr_2O_3 (13) and 2.90 Å found in Fe_2O_3 (14).

There is also a considerable repulsion of metal atoms M_1 and M_2 across the shared edge with $M_1–M_2 = 3.37$ Å. This is to be compared with a value of 2.8 Å calculated for ideal hexagonal close packing, or the average of 2.95 Å for similar edge sharing in Cr_2O_3 and Fe_2O_3. The M–M edge-shared separations for M_4 (2.93 and 3.06 Å) and M_5 (2.94 and 3.11 Å) are much closer to the ideal value.

For the metal atom M_5, associated with the α-PbO_2 fragment of the structure, the M–O and O–O distances are comparable with those in the brookite form of TiO_2 (15) which has the same zigzag strings of edge-shared octahedra. In particular there is one very short O–O distance of 2.48 Å comparable with an O–O distance of 2.49 Å in brookite.

Discussion

The structure of $CrFeTi_2O_7$ may be considered to derive from the α-PbO_2 structural type (see Fig. 2(ii)) by the application of crystallographic shear, parallel to $(110)_{α-PbO_2}$. If we remove every 15th and 16th layer of oxygen atoms parallel to $(110)_{α-PbO_2}$ and displace the adjacent α-PbO_2 slabs by $\frac{1}{2}[010]_{α-PbO_2}$ to collapse the structure, we obtain that shown in Fig. 3. At the shear section of this structure there is a high density of metal atoms in octahedra sharing faces and edges. Repulsion of the metal atoms across the shared faces and edges would introduce strain. One method of relieving such strain would be for alternate $[\bar{1}10]_{α-PbO_2}$ rows of metal atoms at one face of the shear slab to move into adjacent rows of interstices. This results in the formation of the structure of $CrFeTi_2O_7$, shown in Fig. 2(i).
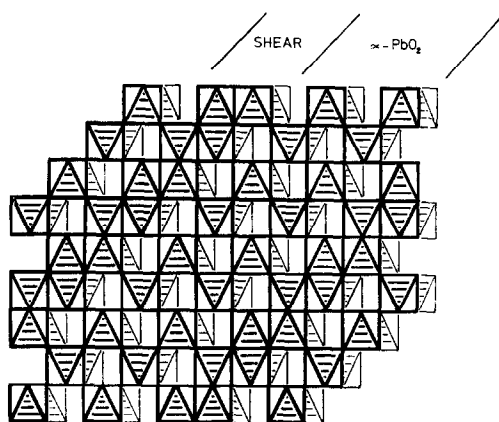

FIG. 3. Idealized representation of a hypothetical structure derived from the α-PbO_2 structure type by crystallographic shear $\frac{1}{2}[010](110)/_{α-PbO_2}$. This represents an intermediate step between α-PbO_2 structure type and the ideal structure (ignoring disorder) found for $CrFeTi_2O_7$.

We have previously described this combination of the shear operation $\frac{1}{2}[010](110)_{α-PbO_2}$ plus rearrangement of alternate rows of metal atoms at the shear interface, as a step shear (16). It is possible to describe an homologous series of compounds, $A_2B_{n-2}O_{2n-1}$, based on the application of this step shear to the α-PbO_2 structure type. $CrFeTi_2O_7$ (A = Cr, Fe, B = Ti) is a member of this series, $n = 4$. The compound V_3O_5 is a representative for $n = 3$ (A = V; B = V). For A = Cr, Fe, B = Ti we have prepared examples of homologues for $n = 3$, 4 and 5 (16); and for A = Cr, Fe, B = Ti, Zr, homologues with $n \geqslant 6$ have been prepared (unpublished). Adjacent members $A_2B_{n-2}O_{2n-1}$ also form ordered intergrowth phases (16).

The preceding description of the structure of $CrFeTi_2O_7$ relates to the ideal structure, with no disorder of the metal atom at site M_1. The 15% disorder actually observed is possibly an indication of incomplete equilibrium of the sample, frozen in by the rapid cooling from 1500°C to room temperature. One possible origin of this disorder is the presence of small amounts of intergrowth phases close to $CrFeTi_2O_7$ (abbreviated M_4O_7) in composition, e.g., $(M_4O_7)_n$ $(M_3O_5)_m$, $n \gg m$. Evidence for small amounts of such intergrowth phases has in fact been found by examination of fragments of $CrFeTi_2O_7$ by selected area electron diffraction.

A second possible origin of the disorder is the freezing in of part of an intermediate, less stable, structure. In Fig. 3 is represented in

idealized form the structure which would result from complete disorder of metal atoms M$_1$ from sites M$_1$ to M$_3$, assuming the space group restrictions imposed by the ideal structure to be obeyed. This structure may be considered to derive from that of α-PbO$_2$ by application of the shear vector $\frac{1}{2}[010](110)_{\alpha\text{-PbO}_2}$ as described above. The disorder actually observed in CrFeTi$_2$O$_7$ could be explained by incomplete conversion from such an unstable, intermediate structure (Fig. 3) to that shown in Fig. 2(i).

Acknowledgments

References

1. M. HAMELIN, *Bull. Soc. Chim. Fr.*, 1421 (1957).
2. S. ANDERSSON, A. SUNDHOLM, AND A. MAGNÉLI, *Acta Chem. Scand.* **13**, 989 (1959).
3. W. KWESTROO AND A. ROOS, *J. Inorg. Nucl. Chem.* **13**, 325 (1960).
4. O. W. FLÖRKE AND C. W. LEE, *J. Solid State Chem.* **1**, 445 (1970).
5. S. ANDERSSON, B. COLLEN, U. KUYLENSTIERNA, AND A. MAGNÉLI, *Acta Chem. Scand.* **11**, 1641 (1957).
6. G. ANDERSSON, *Acta Chem. Scand.* **8**, 1599 (1954).
7. A. D. WADSLEY, *in* "Nonstoichiometric Compounds" (L. Mandelcorn, Ed.), p. 98, Academic Press, New York (1964).
8. J. J. DALY, F. S. STEPHENS, AND P. J. WHEATLEY, Monsanto Research, S.A. Final Report No. 52 (1963).
9. S. ASBINK, S. FRIBERG, A. MAGNÉLI, AND G. ANDERSSON, *Acta Chem. Scand.* **13**, 603 (1959).
10. A. I. ZASLEVSKIJ AND S. S. TOLKACEV, *Zh. Fiz. Khim.* **26**, 743 (1952).
11. N. A. BENDELLIANY, S. V. POPOVA, AND L. F. VERESHCHAGIN, *Geokhimiya*, 499 (1966).
12. R. D. SHANNON AND C. T. PREWITT, *Acta Crystallogr.* **B25**, 925 (1969).
13. R. E. NEWNHAM AND Y. M. DE HAAN, *Z. Kristallogr. Kristallgeom. Kristallphys. Kristallchem.* **117**, 235 (1962).
14. R. L. BLAKE, R. E. HESSEVICK, T. ZOLTAI, AND L. W. FINGER, *Amer. Mineral.* **51**, 123 (1966).
15. W. H. BAUR, *Acta Crystallogr.* **14**, 214 (1961).
16. I. E. GREY AND A. F. REID, *J. Solid State Chem.* **4**, 186 (1972).
17. S. ANDERSSON AND J. GALY, *J. Solid State Chem.* **1**, 576 (1970).